Peripheral lymphadenomegaly in a Jack Russell Terrier

Contributors
Argyrios Ginoudis[1], Valeria Martini[2], Dimitra Pardali[1], Avgi Samara[3], Panagiotis Ygeionomakis[3], Eleni-Antonia Mavropoulou[4], Tatiana Rothacker[5], Rania Farmaki[1], Michail Patsikas[4], Mathios E. Mylonakis[3]

[1]Diagnostic Laboratory, School of Veterinary Medicine, Faculty of Health Sciences, Aristotle University of Thessaloniki, Thessaloniki, Greece
[2]Department of Veterinary Medicine and Animal Sciences, University of Milan, Lodi, Italy
[3]Companion Animal Clinic (Medicine Unit), School of Veterinary Medicine, Faculty of Health Sciences, Aristotle University of Thessaloniki, Thessaloniki, Greece
[4]Laboratory of Diagnostic Imaging, School of Veterinary Medicine, Faculty of Health Sciences, Aristotle University of Thessaloniki, Thessaloniki, Greece
[5]IDEXX Vet Med Labor, Kornwestheim, Germany

Argyrios Ginoudis: agkinou@vet.auth.gr

Specimen
Peripheral lymph node aspirates (cytology smears, RPMI 1640-preserved specimens), lung aspirates, EDTA whole blood.

Signalment
Dog, Jack Russell Terrier, 13 years old, male neutered.

History
Referred for investigation of generalized lymphadenomegaly that was noticed two weeks prior to admission.

Clinical findings
The dog was bright, alert, and responsive but exhibited generalized severe lymphadenomegaly and hepatosplenomegaly. A complete blood count (ADVIA® 2120 Hematology System, Siemens Healthineers, Malvern, PA, USA) revealed moderate thrombocytopenia which was confirmed with a blood smear examination where no platelet clumps were seen (Table 1). Serum biochemistry was unremarkable. A serological point-of-care ELISA test (SNAP Leish 4Dx test, IDEXX Laboratories Inc., Westbrook, ME, USA) for *Leishmania infantum*, *Ehrlichia* spp. and *Anaplasma* spp. antibodies and *Dirofilaria immitis* antigen was negative.

Fine-needle aspirates were obtained from the submandibular, prescapular, axillary, and popliteal lymph nodes and submitted for cytological evaluation (Figures 1-6).

Extensive soft tissue diffuse opacities were identified in the left lung on plain radiographs. Ultrasound-guided aspiration of the pulmonary lesions was performed and submitted for cytological evaluation (Figures 7-10). Abdominal ultrasonography indicated severe enlargement of hepatic lymph nodes. Moderate mesenteric lymphadenopathy, and mild gastric and internal iliac lymphadenomegaly was also noted. The spleen exhibited moderate splenomegaly with diffuse hypoechogenicity.

The thoracic CT scan revealed severe enlargement of the sternal, tracheobronchial, and mediastinal lymph nodes. Consolidation was noted in the caudal part of the left cranial

lung lobe, with alveolar-pattern infiltrates and extensive areas of complete loss of aeration (Figure 11).

Questions

1. What is your cytologic description of the lymph node and pulmonary aspirates?
2. What are the main differential diagnoses based upon cytologic examination?
3. Which are the next steps in the diagnostic investigation?

Table 1. Complete Blood Count (ADVIA® 2120 Hematology System, Siemens Healthineers, Malvern, PA, USA)

Parameter	*Value*	*Reference Interval*
Red blood cells (x10^9/µL)	**5.41**	**5.50-8.50**
Hemoglobin (g/dL)	14.2	12.0-18.0
Hematocrit (%)	42.2	37.1-55.0
Mean corpuscular volume (fL)	**78.1**	**60.6-77.0**
Mean Corpuscular Hemoglobin Concentration (g/dL)	33.6	31.0-36.2
Red Cell Distribution Width (%)	13.7	11.9-14.5
Reticulocytes (x10^3/µL)	99.1	10.0-110.0
White Blood Cells (x10^3/µL)	11.6	6.0-17.0
Neutrophils (x10^3/µL)	7.1	3.9-8.0
Lymphocytes (x10^3/µL)	3.5	1.3-4.1
Monocytes (x10^3/µL)	0.6	0.2-1.1
Eosinophils (x10^3/µL)	0.29	0.00-0.60
Basophils (x10^3/µL)	0.03	0.00-0.10
Large Unstained Cells (x10^3/µL)	0.06	0.00-0.30
Platelets (x10^3/µL)	**117**	**200-500**
Mean Platelet Volume (fL)	**11.6**	**5.4-9.2**

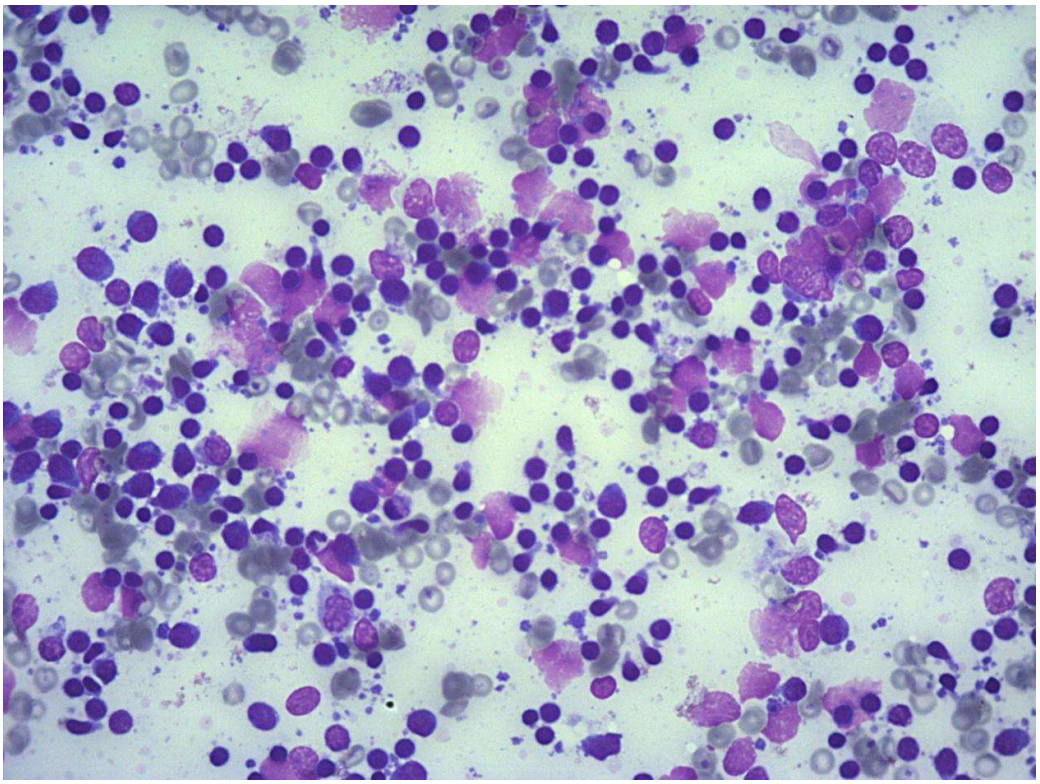

Figure 1. Fine needle aspirate of the right submandibular lymph node (x400, Giemsa)

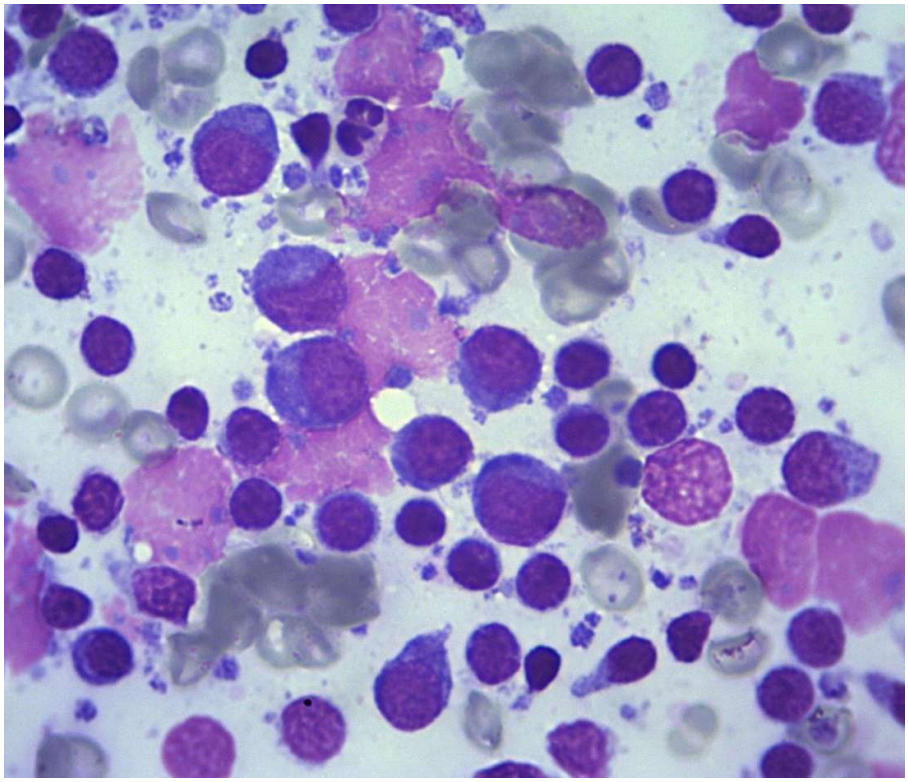

Figure 2. Fine needle aspirate of the right submandibular lymph node (x1000, Giemsa)

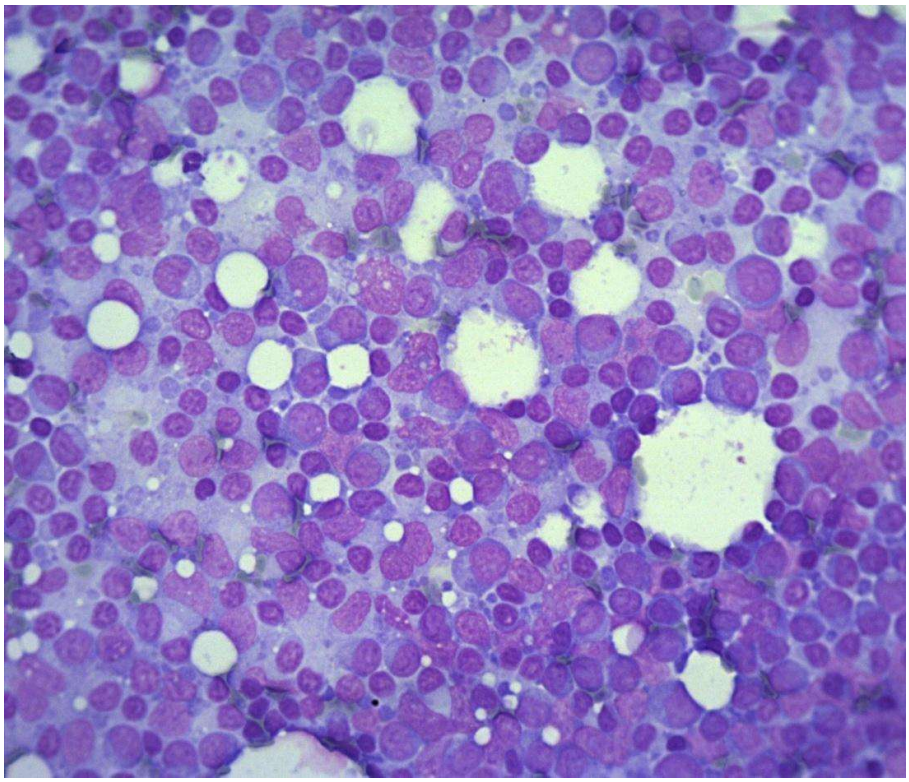

Figure 3. Fine needle aspirate of the left popliteal lymph node (x400, Giemsa)

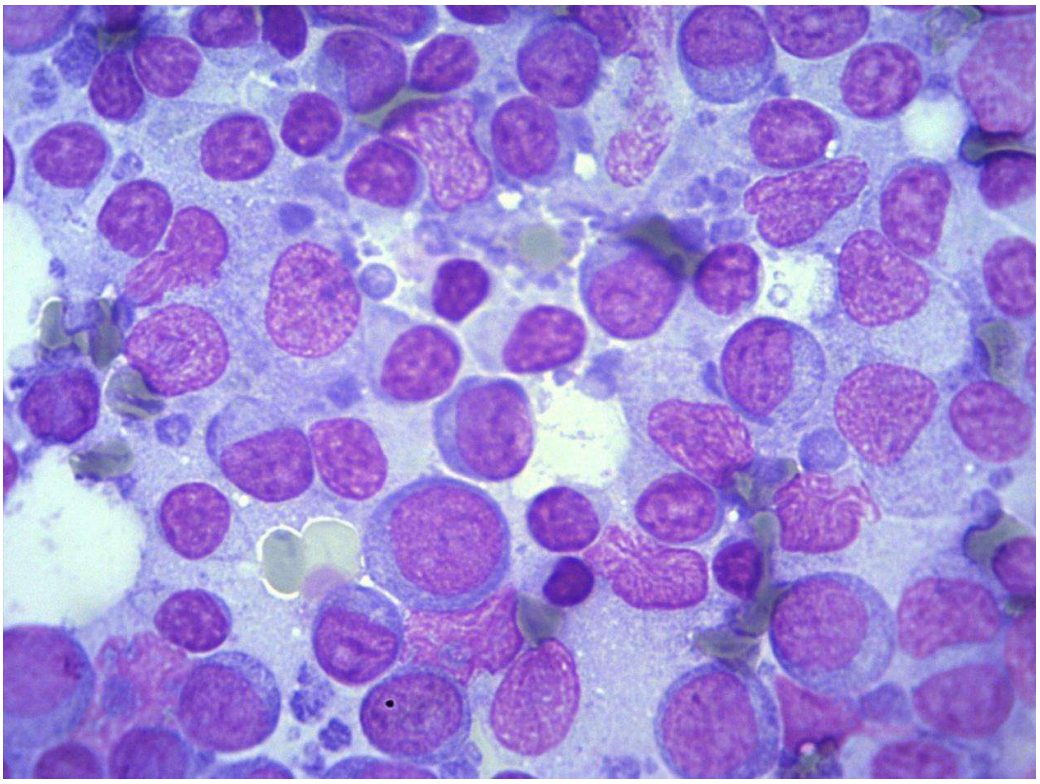

Figure 4. Fine needle aspirate of the left popliteal lymph node (x1000, Giemsa)

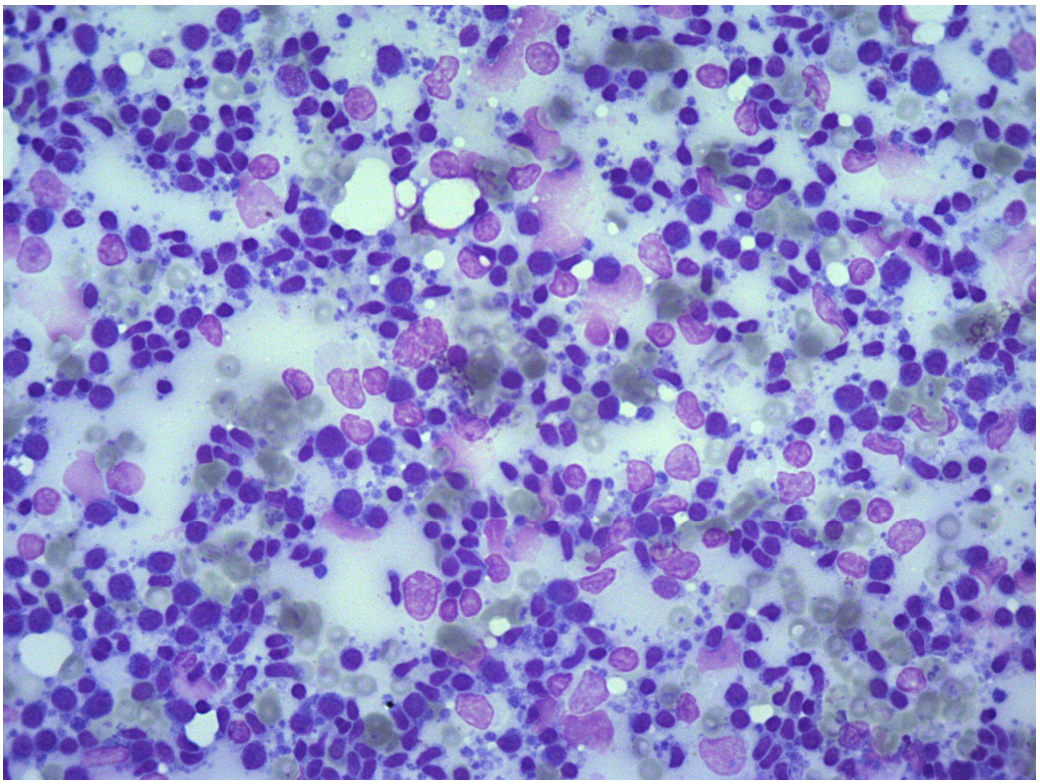

Figure 5. Fine needle aspirate of the right popliteal lymph node (x400, Giemsa)

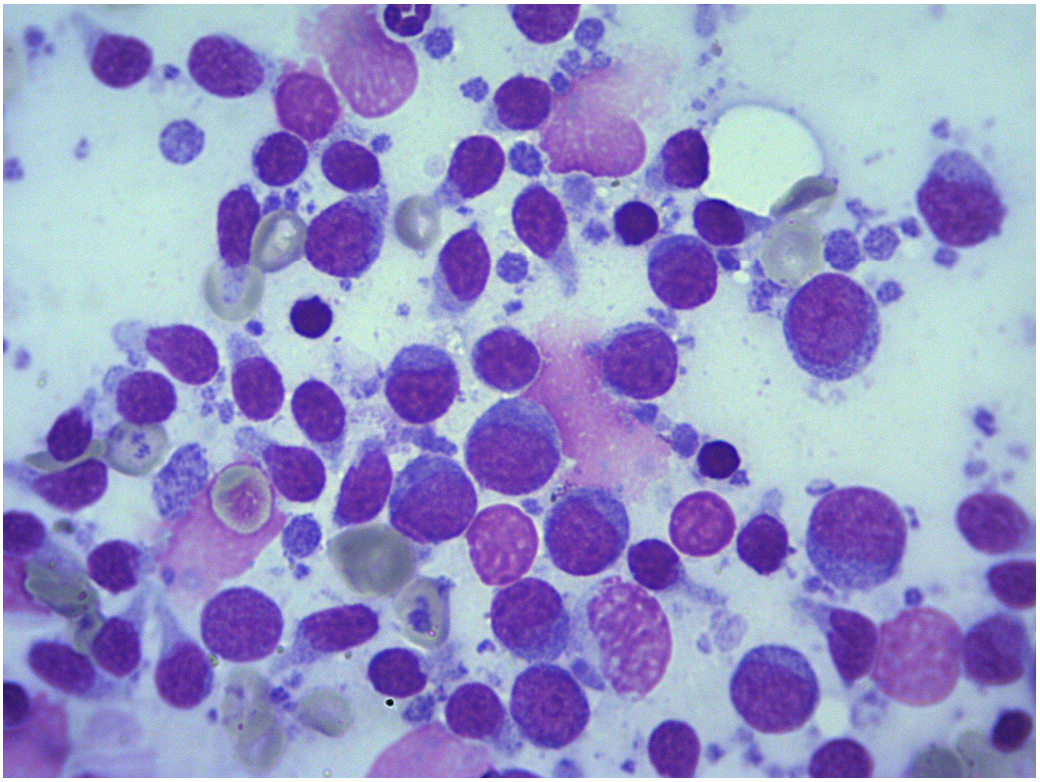

Figure 6. Fine needle aspirate of the right popliteal lymph node (x1000, Giemsa)

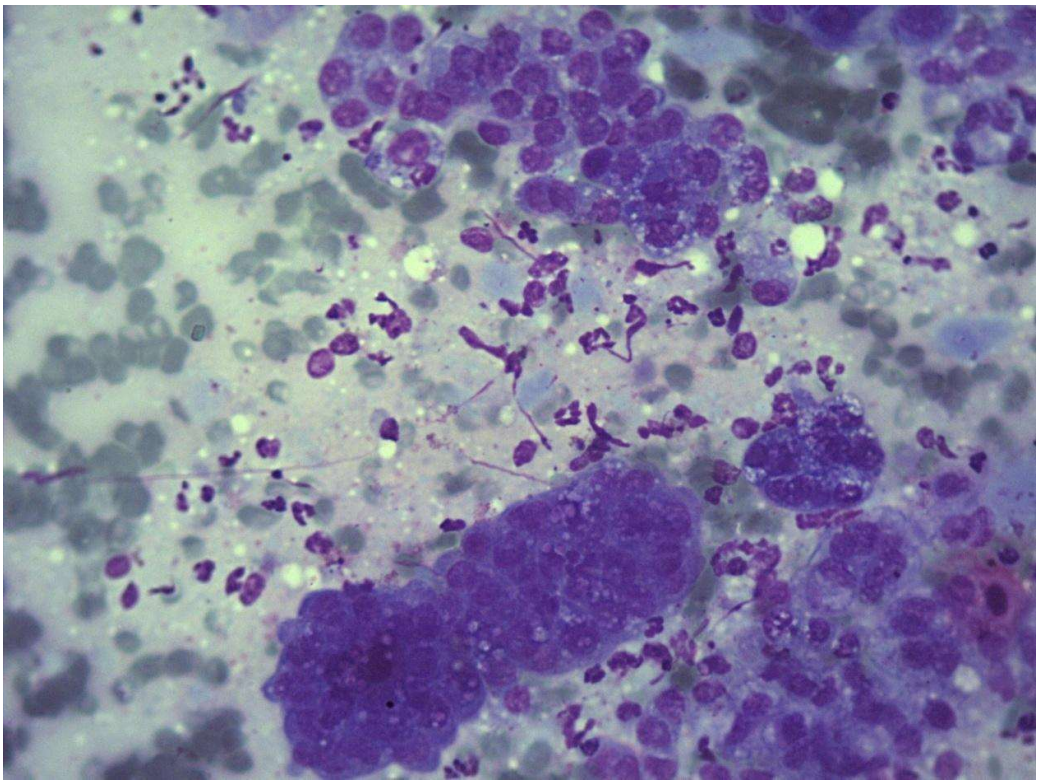

Figure 7. Fine needle aspirate of the pulmonary lesions (x400, Giemsa)

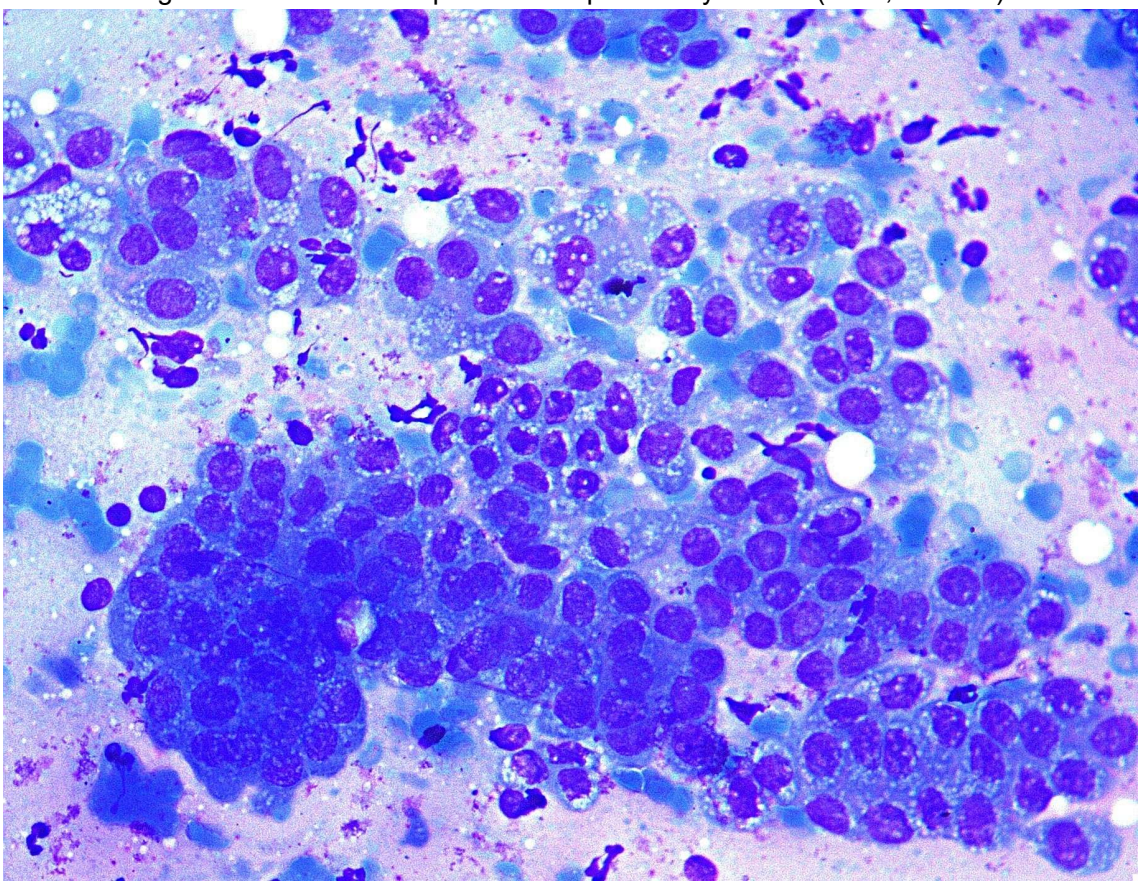

Figure 8. Fine needle aspirate of the pulmonary lesions (x400, Giemsa)

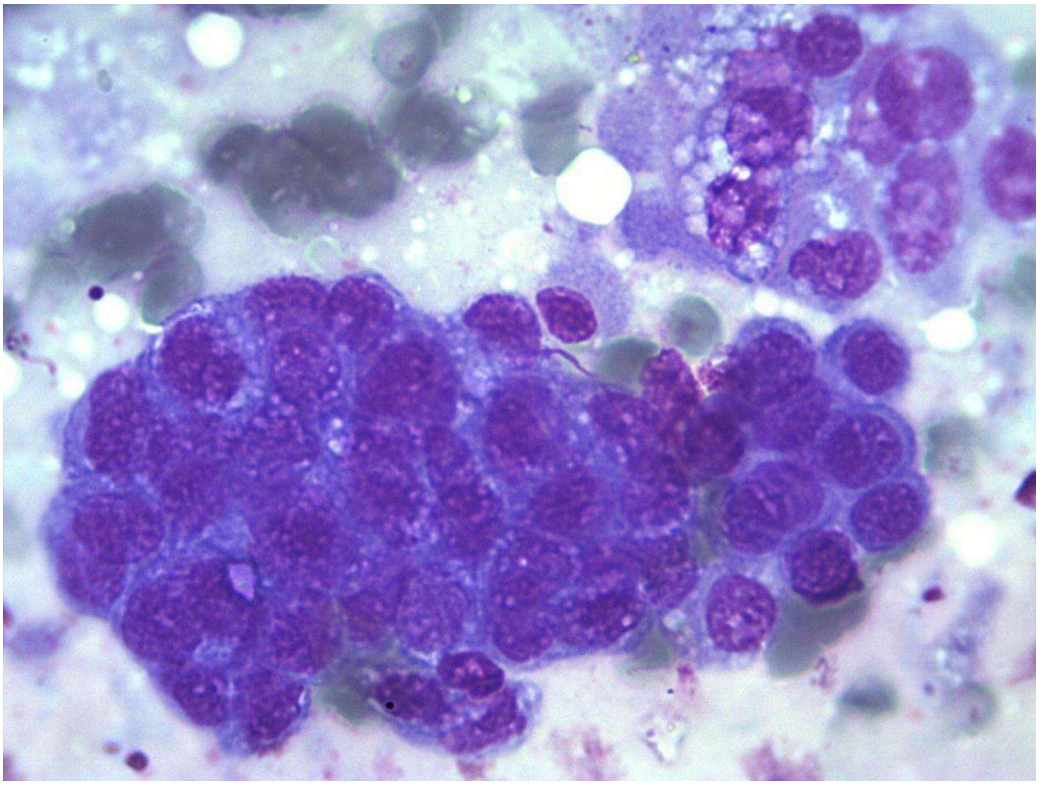

Figure 9. Fine needle aspirate of the pulmonary lesions (x1000, Giemsa)

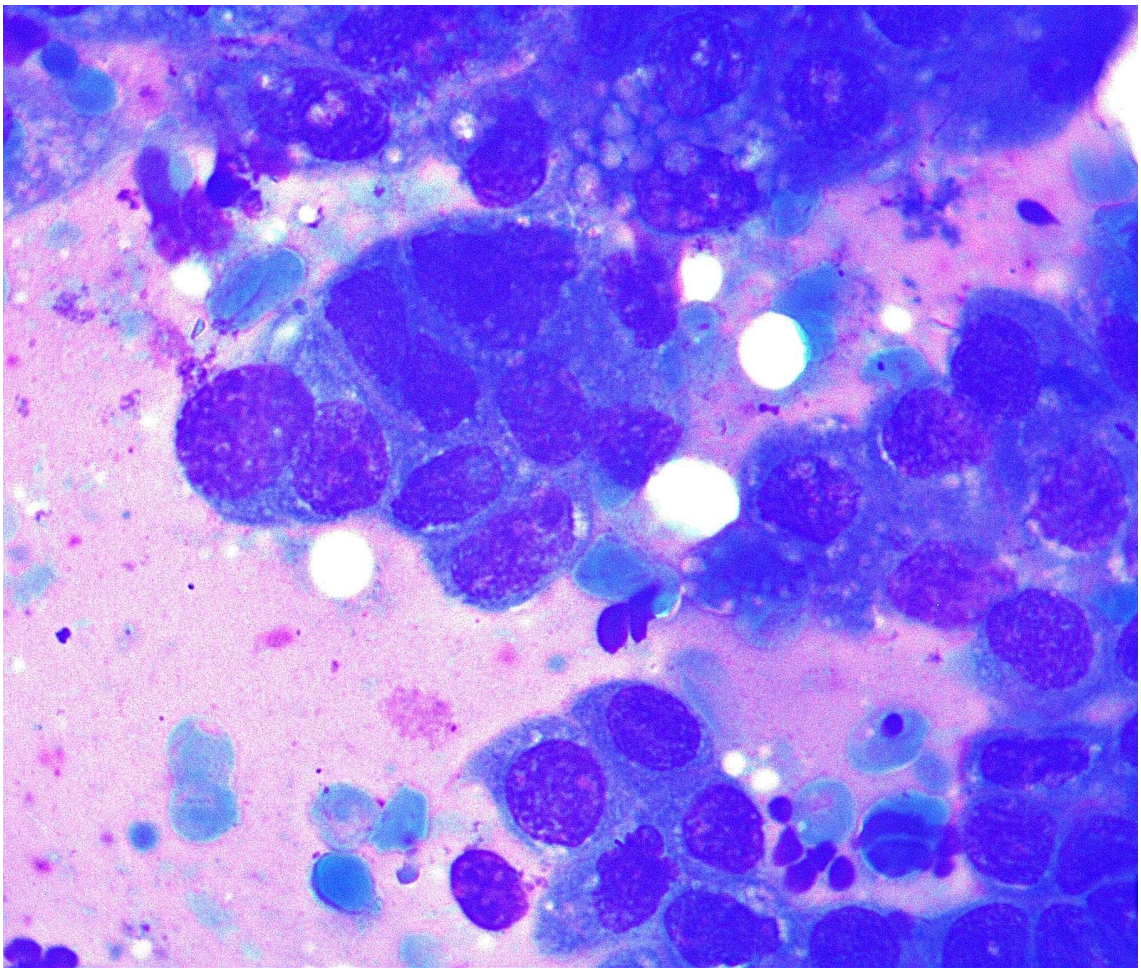

Figure 10. Fine needle aspirate of the pulmonary lesions (x1000, Giemsa)

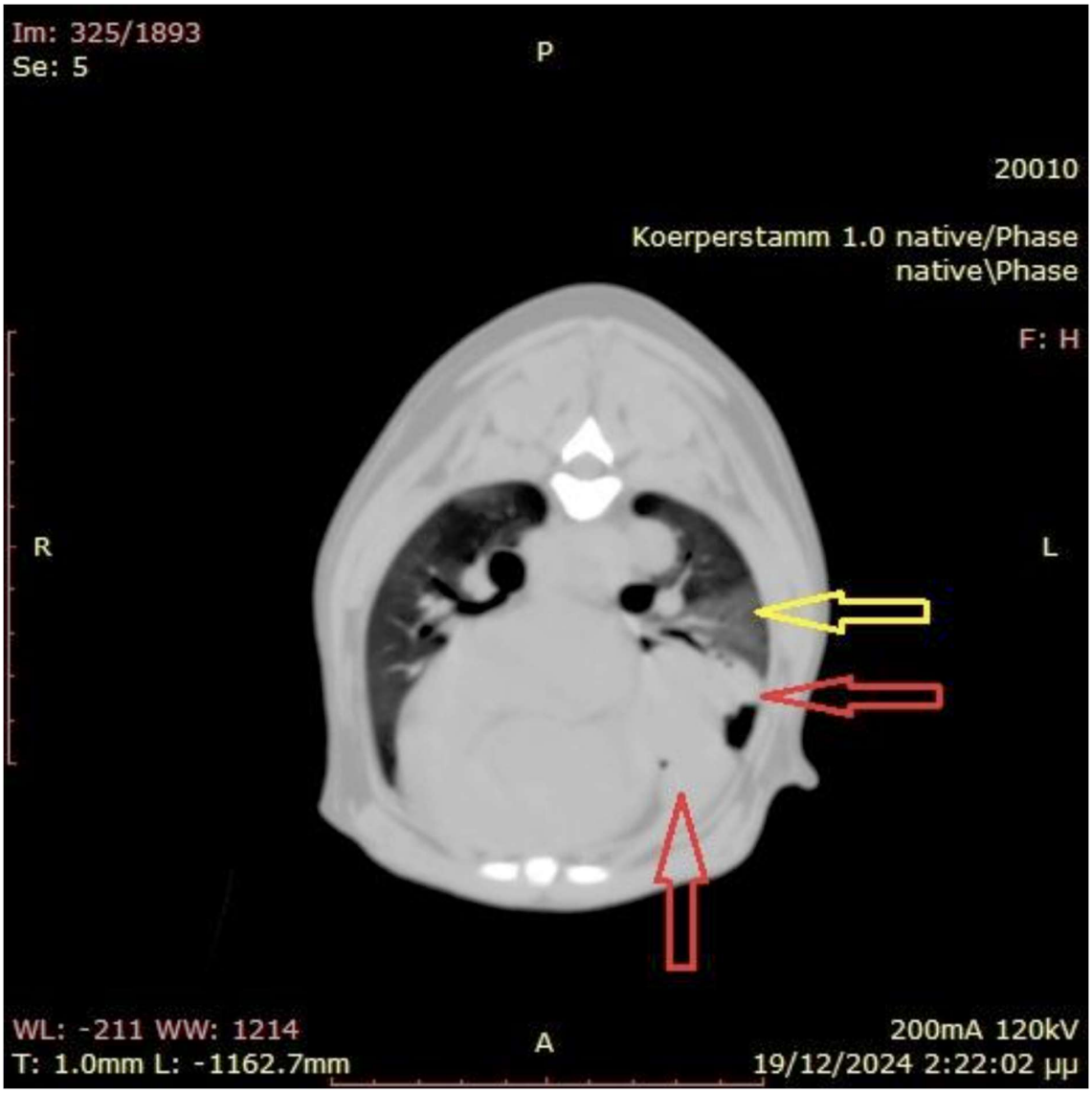

Figure 11. Consolidation of the caudal part of the left cranial lung lobe, with alveolar-pattern infiltrates and extensive areas of complete loss of aeration (red arrows). Associated ground-glass opacities are also noted (yellow arrow).

1. **What is your cytologic description of the lymph node and pulmonary aspirates?**

Cytologic Description

The peripheral lymph node aspirates are of high cellularity and adequate preservation. In many areas, intermediate to large lymphocytes predominate (depicted in Figures 3 and 4), exhibiting round nuclei with finely stippled chromatin, one to three distinct nucleoli, and a small amount of variably basophilic cytoplasm. A distinct population of small to intermediate lymphocytes with small amounts of pale basophilic cytoplasm with cytoplasmic extensions (hand-mirror shaped) is predominant in many areas of all aspirates, particularly the popliteal and submandibular lymph nodes.

The aspirates of the pulmonary lesions revealed a population of atypical cuboidal to round cells arranged in cohesive clusters of tubular or acinar arrangements. They exhibited mild to moderate anisocytosis and anisokaryosis, increased nuclear-to-cytoplasmic ratio, irregularly round to oval nuclei with a finely stippled chromatin pattern, and a moderate amount of basophilic, vacuolated cytoplasm. A mild neutrophilic infiltration was noted. Cytological findings combined with CT findings were consistent with an epithelial neoplasia (likely primary or metastatic lung adenocarcinoma).

2. **What are the main differential diagnoses based upon cytologic examination?**
   - Intermediate-large cell lymphoma with concurrent T zone lymphoma (TZL) and pulmonary epithelial neoplasia,
   - Intermediate-large cell lymphoma with T-zone hyperplasia and pulmonary epithelial neoplasia,
   - TZL with lymphoid hyperplasia and pulmonary epithelial neoplasia.

3. **Which are the next steps in the diagnostic investigation?**
   - Flow cytometry of lymph node aspirates and whole blood to immunophenotype the cell populations and investigate blood infiltration.
   - PCR for Antigen Receptor Rearrangement (PARR) to assess clonality of the lymphoid population.
   - Lymph node histopathology to further classify the lymphomas.

Additional information

Flow cytometry

Flow cytometry of the popliteal lymph nodes on presentation revealed a population that consists mainly of lymphoid cells staining negative for CD45, positive for CD5, CD21 and MHCII, and negative for CD4 and CD8. Most of these cells were small to intermediate, but a small subset (2%) of cells with the same phenotype and large size is present. In addition, there is a distinct population (20%) of intermediate to large cells staining positive for CD21 and MHCII (Table 2).

Table 2. Flow cytometry of popliteal lymph node aspirates on presentation.

Gating strategy	Percentage
CD45	40.2%
CD5	76.1%
CD4	8.7%
CD8	2.1%
CD21	85.7%
MHC II	90.4%
CD34	0.2%

Based on these results, three different lymph node aspirates (submandibular, prescapular and popliteal), together with a peripheral blood sample were tested again via flow cytometry one week post presentation. Based on the previous results, only CD45, CD5 and CD21 antibodies were tested.

In all four matrices, two different populations were found (Table 3). The first one consisted of small to intermediate lymphoid cells with CD45-/CD5+ phenotype, and accounted for 47%, 38% and 53% of all nucleated cells in the three different nodal aspirates, respectively, and for 12% in the peripheral blood sample. The second population consisted of intermediate to large lymphoid cells with CD21+/CD45+ phenotype, and accounted for 35%, 38% and 17% of all nucleated cells in the three different nodal aspirates, respectively, and for 1.4% in the peripheral blood sample.

The first population was considered suggestive of infiltration by T-zone lymphoma in all matrices tested. The second one was suggestive of B-cell lymphoma in the submandibular and prescapular lymph node aspirates, with blood infiltration. The percentage of cells detected in the popliteal lymph node aspirate could not be considered suggestive of neoplasia, being <20%. Still, based on the findings on the remaining matrices, that sample was considered strongly suspected for infiltration by B-cell lymphoma.

Table 3. Flow cytometry of peripheral blood and lymph node aspirates.

Gating strategy	Peripheral blood	Submandibular lymph nodes	Prescapular lymph nodes	Popliteal lymph nodes
CD45-/CD5+ cells	12.0%	47.0%	38.0%	53.0%
intermediate/large CD21+ cells	1.4%	35.0%	38.0%	17.0%

PARR in lymph node aspirates

The PARR test identified clonal BCR gene rearrangement and clonal TCR gene rearrangement on a polyclonal background, indicating the presence of both a neoplastic and a reactive lymphoid population (Figure 12). These findings, when correlated with cytology and flow cytometry results (CD5+/CD45- cells and a population of large CD21+ cells), support a diagnosis of dual small-cell T-zone lymphoma and large B-cell lymphoma.

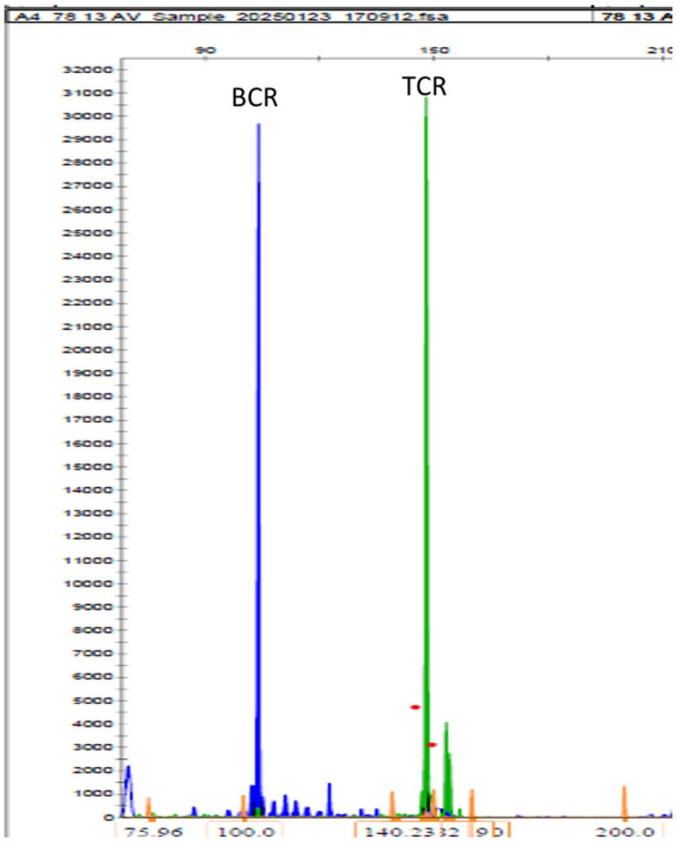

Figure 12. PARR electropherogram showing clonal peaks in the B-cell receptor (BCR, blue) and T-cell receptor (TCR, green) gene regions, indicative of B- and T-cell clonality.

Follow-up and clinical outcome

Lymph node histopathology was recommended to better characterize the lymphomas and determine the most appropriate chemotherapeutic protocol. However, the owner declined this option. Since the pulmonary lesions were deemed inoperable, chemotherapy with toceranib (2.7 mg/kg orally, three times per week) was initiated. After three weeks of treatment, progression of pulmonary disease occurred (the dog developed respiratory distress, and increased coughing episodes). Consequently, treatment was switched to doxorubicin (1 mg/kg intravenously every 21 days), which led to a partial reduction in lymph node size and partial relief of respiratory symptoms. As of this writing, 6 months post-admission, the dog is doing well.

Discussion

This report describes a rare case of presumptive dual lymphoma in a dog, involving a combination of TZL and large B-cell lymphoma (LBCL) involving multiple superficial and cavitary lymph nodes. The coexistence of two distinct types of lymphoma is characterised as composite lymphoma in human medicine, representing 1-4% of lymphomas (Thirumala et al, 2000) and has rarely been reported in dogs.

The diagnosis of TZL was supported by cytology, which revealed a distinct population of small to intermediate lymphocytes with hand-mirror–shaped cytoplasmic projections, a characteristic feature of TZL. Flow cytometry identified a population of CD5+/CD45- cells, which is diagnostic for this type of T-cell lymphoma, when combined with the cytological appearance (Martini et al, 2015; Martini et al, 2016). T-zone hyperplasia is highly unlikely in this case, considering the CD45- cells and the clonal expansion of T cells. Canine ehrlichiosis (*Ehrlichia canis*) is also unlikely, as this dog was seronegative and typically a T-cell expansion affects the CD8 cells, which in this case were not increased. TZL is an indolent lymphoma with a reported median survival time of 637-760 days (Seelig et al, 2014; Martini et al, 2015), with or without chemotherapy.

Concurrently, the presence of intermediate to large CD21+ lymphocytes in multiple lymph nodes strongly suggested a LBCL, in agreement with cytological presentation of many areas with predominance of intermediate and large lymphocytes (Gelain et al, 2008). The dual lymphoma was further supported by PARR results, which demonstrated the coexistence of two distinct clonal lymphocyte populations on a polyclonal background.

However, PARR is not entirely definitive in characterizing neoplastic cells and should be interpreted alongside cytology and flow cytometry results (Waugh et al, 2016). Additionally, histopathology would have been essential in this case, as it would have further characterized the subtype of the LBCL, although the presence of LBCL in dogs is virtually always considered as a diffuse LBCL (DLBCL) (Valli et al., 2010). However, the presence of a rare subtype of LBCL such as nodal marginal zone lymphoma, Burkitt-like lymphoma or follicular lymphoma cannot be confidently ruled out without lymph node histopathology (Wolf-Ringwald et al, 2020). The absence of histopathologic confirmation remains a limitation in this case, as it could have provided more precise classification and prognostic insights.

While the dual lymphoma diagnosis was significant, the identification of an independent pulmonary neoplasia was considered a more direct threat to the patient. Cytology of the pulmonary lesion showed cohesive clusters of atypical epithelial cells, consistent with an epithelial malignancy. Given the aggressive nature of this lesion and its probable contribution to the patient's respiratory symptoms, treatment decisions were largely influenced by the need to address the epithelial neoplasia in addition to the lymphomas.

A CHOP-based protocol would be the chemotherapeutic approach of choice to target the LBCL as the most aggressive of the two lymphoma types (Vail et al, 2019). However, this was not pursued due to concerns that it would not adequately target the epithelial neoplasia, which posed a more immediate threat to the patient. This case highlights the complexities of managing multiple concurrent malignancies, particularly when different neoplastic processes require distinct therapeutic approaches. The presence of both an indolent lymphoma (TZL) and a potentially aggressive lymphoma (LBCL) already posed challenges in selecting an optimal treatment strategy, but the additional presence of an epithelial pulmonary neoplasia necessitated a significant deviation from standard lymphoma protocols.

Composite lymphomas have already been reported in dogs, with concomitant diagnosis of circulating TZL and nodal LBCL (Long et al, 2020; Rosenbaum et al, 2021): in both cases, large B-cells were the prevalent population in LN aspirates, thus being diagnostic for LBCL, although molecular clonality was not assessed in one case (Long et al, 2020). Also Matsuyama et al. (2019), have demonstrated the coexistence of TZL and LBCL. In their case, the dog initially presented with TZL, and 13 months later developed a distinct, clonally unrelated LBCL, confirmed through next-generation sequencing (NGS)-based clonality testing. This method definitively demonstrated that the two neoplasms arose independently rather than through transformation, highlighting the importance of molecular testing in differentiating multiple lymphoid neoplasms. In particular, cytology and flow cytometry might be not enough to differentiate composite lymphomas from Richter's syndrome, which is the transformation of chronic leukemia (CLL) into an aggressive form of lymphoma, typically DLBCL (Comazzi et al., 2017). Our case differed from those already published in that both lymphoma populations were present on admission, together with a third, unrelated neoplasm (pulmonary adenocarcinoma), and in that the proportion of large B-cells was not prevalent in either lymph node aspirate, thus requiring PARR to definitively confirm the neoplastic nature of this population.

Conclusion

This case underscores the challenges of diagnosing complex lymphoid malignancies using cytology alone, particularly when different neoplastic populations are present in varying distributions across slide preparations. Careful microscopic examination of multiple areas was necessary to identify both the intermediate-large B-cell population and the small to intermediate T-zone lymphocytes, highlighting the potential for misdiagnosis if only focal areas are assessed. The integration of flow cytometry and PARR were crucial in confirming the presence of a dual lymphoma, as immunophenotyping and molecular testing provided definitive differentiation between the B-cell and T-cell populations. This case emphasizes the importance of using a multimodal diagnostic approach, including cytology, histopathology, flow cytometry, and molecular testing, to accurately characterize lymphoid malignancies, especially in cases where cytologic findings are heterogeneous.

References

1. Comazzi S, Martini V, Riondato F, Poggi A, Stefanello D, Marconato L, Albonico F, Gelain ME. Chronic lymphocytic leukemia transformation into high-grade lymphoma: a description of Richter's syndrome in eight dogs. Veterinary and comparative oncology 2017; 15: 366–373. https://doi.org/10.1111/vco.12172
2. Gelain ME, Mazzilli M, Riondato F, Marconato L, Comazzi S. Aberrant phenotypes and quantitative antigen expression in different subtypes of canine lymphoma by flow

cytometry. Veterinary immunology and immunopathology 2008; 121: 179–188. https://doi.org/10.1016/j.vetimm.2007.09.018
3. Long ME, Evans B, Avery AC, Wellman, ML. Lymphocytosis and lymphadenopathy in a dog arising from two distinct lymphoid neoplasms. Veterinary clinical pathology 2020; 49: 307–311. https://doi.org/10.1111/vcp.12855
4. Martini V, Poggi A, Riondato F, Gelain ME, Aresu L, Comazzi S. Flow-cytometric detection of phenotypic aberrancies in canine small clear cell lymphoma. Veterinary and comparative oncology 2015; 13: 281–287. https://doi.org/10.1111/vco.12043
5. Martini V, Marconato L, Poggi A, Riondato F, Aresu L, Cozzi M, Comazzi S. Canine small clear cell/T-zone lymphoma: clinical presentation and outcome in a retrospective case series. Veterinary and comparative oncology 2016; 14: 117–126. https://doi.org/10.1111/vco.12155
6. Matsuyama A, Bienzle D, Richardson D, Deravi N, Hwang M H, Darzentas N, Keller SM. Composite lymphoma of concurrent T zone lymphoma and large cell B cell lymphoma in a dog. BMC veterinary research 2019; 15: 413. https://doi.org/10.1186/s12917-019-2154-8
7. Rosenbaum CS, Seelig DM, Burton EN, Gwynn AD, Granick J, Able HR. Monitoring of large B-cell lymphoma and T-zone lymphoma in a dog via flow cytometry. Journal of Veterinary Diagnostic Investigation. 2021; 33: 1008-1012. https://doi.org/10.1177/10406387211027162
8. Seelig DM, Avery P, Webb T, Yoshimoto J, Bromberek J, Ehrhart EJ, Avery AC. Canine T-zone lymphoma: unique immunophenotypic features, outcome, and population characteristics. Journal of veterinary internal medicine, 2014, 28, 878–886. https://doi.org/10.1111/jvim.12343
9. Thirumala S, Esposito M, Fuchs A. An unusual variant of composite lymphoma: a short case report and review of the literature. Archives of pathology & laboratory medicine 2000; 124; 1376–1378. https://doi.org/10.5858/2000-124-1376-AUVOCL
10. Vail DM, Thamm D, Liptak J. Withrow and MacEwen's Small Animal Clinical Oncology. 6th ed. St Louis, MO: Elsevier; 2019.
11. Valli VE, Myint MS, Barthel A, et al. Classification of Canine Malignant Lymphomas According to the World Health Organization Criteria. Veterinary Pathology 2010; 48: 198-211. https://doi.org/10.1177/0300985810379428
12. Waugh EM, Gallagher A, Haining H, Johnston PEJ, Marchesi F, Jarrett RF, Morris JS. Optimisation and validation of a PCR for antigen receptor rearrangement (PARR) assay to detect clonality in canine lymphoid malignancies. Veterinary immunology and immunopathology 2016; 182: 115–124. https://doi.org/10.1016/j.vetimm.2016.10.008
13. Wolf-Ringwall A, Lopez L, Elmslie R, Fowler B, Lori J, Sfiligoi G, Skope A, Arnold E, Hughes KL, Thamm DH, Ehrhart EJ 3rd, Avery AC, Lana, SE. Prospective evaluation of flow cytometric characteristics, histopathologic diagnosis and clinical outcome in dogs with naïve B-cell lymphoma treated with a 19-week CHOP protocol. Veterinary and comparative oncology 2020; 18: 342–352. https://doi.org/10.1111/vco.12553